Viscoelastic Kelvin-Helmholtz instability

T. W. Searle[1] and A. N. Morozov[1]†,

[1]SUPA, School of Physics and Astronomy, University of Edinburgh, Mayfield Road, Edinburgh, EH9 3JZ, UK

(Received ?; revised ?; accepted ?. - To be entered by editorial office)

Abstract goes here. Abstract goes here. Viscoelastic Kelvin-Helmholtz instability.

Key words: Authors should not enter keywords on the manuscript, as these must be chosen by the author during the online submission process and will then be added during the typesetting process (see http://journals.cambridge.org/data/relatedlink/jfm-keywords.pdf for the full list)

---

1. Introduction

Turbulence without inertia in viscoelastic fluids has generated much interest since it was discovered in Taylor-Couette flow by Larson, Shaqfeh and Muller in 1990 Larson *et al.* (1990). As well as this numerical and experimental study of Taylor-Couette flow, Groisman and Steinberg Groisman & Steinberg (2000) discovered turbulence in viscoelastic fluids between two counter rotating plates.

It was long thought that the elasticity of a viscoelastic fluid only served to dampen instability. This view stems from early results showing that drag in a turbulent Newtonian flow can be reduced by the addition of small amounts of viscoelastic fluid (Toms (1977)). Although drag reduction has received a lot of attention in the past, studies on turbulence without inertia give reason to believe that there may be purely elastic instabilities present in elastic fluids relevent to industry. This purely elastic turbulence is present at very low Reynolds number, where it is driven by the elasticity of the polymeric fluid rather than its inertia.

In 1997 Fabian Waleffe identified a Newtonian self sustaining process in plane Couette flow Waleffe (1997). Streamwise rolls redistribute the streamwise velocity into a streaky flow. This streaky flow is unstable through a Kelvin-Helmholtz instability leading to a symmetry bifurcation to a three dimensional flow. Finally, the nonlinear effects due to this instability re-energises the original streamwise rolls. This exact solution to the Navier-Stokes equations is thought to be a component of the transition to turbulence. In 1998 Waleffe constructed a bifurcation diagram for this exact solution Waleffe (1998) containing what looks like a bifurcation from infinity, just the behaviour expected of the transition to turbulence in plane Couette flow.

Using this work in Newtonian fluid dynamics as a template for the structure of purely elastic turbulence reveals a similar pattern of streaks and, hopefully, a similar self-sustaining process **?**. An important step towards explaining this process in purely elastic flows is establishing the mechanism by which the streaks become unstable. Presumably, this will also be a Kelvin-Helmholtz instability as the streaks shear with the rest of the

† Email address for correspondence: jfm@damtp.cam.ac.uk

fluid. The Kelvin-Helmholtz instability is also often integral to the transition to turbulence in Newtonian fluids. It is hoped that by finding a purely elastic version of this instability, we might be able to probe one of the important mechanisms for the transition to purely elastic turbulence. To explore this mechanism in the purely elastic regime we have constructed a simple model system of a shearing viscoelastic fluid.

The key dimensionless number for turbulence without inertia in viscoelastic flows is the Weissenberg number, which is the ratio of the normal stress to the shear stress of the polymer component of the fluid $Wi = \frac{N_1}{\sigma} = \lambda\dot{\gamma}$ where $\dot{\gamma}$ is the shear rate.

We present a linear stability analysis of the Kelvin-Helmholtz instability in the purely elastic regime using direct numerical simulation of both the Oldroyd-B and FENE-P constitutive models for a polymeric fluid. The purely elastic fluid is found to be unstable at sufficiently high numbers of the dimensionless parameter, the Weissenberg number. The growth rate of the largest growing eigenmode of the instability is found to increase with increasing Weissenberg number for low Reynold's number. This behaviour is consistent across both the Oldroyd-B and FENE-P models.

The system we use for our analysis uses a hyperbolic tangent shaped laminar profile for the streamwise velocity across a channel, where the instability takes place between $y = \pm\Delta$. $y = 0$ is the centreline of the channel, so that if $\Delta << 1$ the flow can be said to be a free shear instability. This gives a base flow profile,

$$\begin{aligned} U(y) &= \tanh(y/\Delta)\coth(1/\Delta) \\ V &= 0 \\ T_{xx}(y) &= 2Wi\left(\frac{\partial U}{\partial y}\right)^2 \\ T_{xy}(y) &= \frac{\partial U}{\partial y} \\ T_{yy}(y) &= 0 \end{aligned}$$

U and V are the base streamwise (x) and wall normal (y) velocities respectively. T is the base stress tensor. We use Gauss-Labatto points in the wall-normal (y) direction for the base profile, and decomposed the disturbances to this flow into Fourier modes.

$$g(y) = \sum_{n=-N}^{N} \widetilde{g}(y)e^{ikx+\lambda t} \tag{1.1}$$

for all disturbance variables $g = u, v, p, \tau_{i,j}$. Where N is the number of Fourier modes, k is the streamwise wavenumber of the disturbance and λ is the growth rate of the mode. This program uses two domains of pseudo-spectral points to give increased resolution in the centre of the simulation. The simulation was also repeated using a code for which the system of points was stretched using:

$$z_u = \frac{y_u}{1 - y_u} \tag{1.2}$$

$$z_b = \frac{y_b}{1 + y_b} \tag{1.3}$$

$$U = \tanh z/\Delta \tag{1.4}$$

This system ought to be completely insensitive to the boundary conditions on the flow and so also behave as a free shear instability.

The dimensionless quantities used throughout are non-dimensionalised relative to the

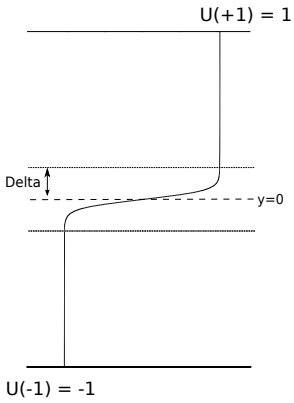

Figure 1: diagram of the system

instability size, Δ, rather than the total simulation size. The obvious reason for this is that Δ is the length scale for the free shear instability.

In order to simulate this flow, we used an Oldroyd-B fluid with very low Reynolds number $Re < 0.01$ and a small ratio between the solvent and total viscosities $\beta = \frac{\mu_s}{\mu_s+\mu_p}$. This approximates a purely elastic fluid, where the polymer contribution to the dynamics is higher than the solvent contribution. The Oldroyd-B Navier stokes and constitutive equations are then:

$$Re\left[\frac{d\mathbf{v}}{dt} + \mathbf{v}\cdot\nabla\mathbf{v}\right] = -\nabla p + \beta\nabla^2\mathbf{v} + \frac{1-\beta}{Wi}\nabla\cdot\tau \tag{1.5}$$

$$\dot{\tau}/Wi + \overset{\nabla}{\tau} = (\nabla\mathbf{v})^T + \nabla\mathbf{v} \tag{1.6}$$

With $\mathbf{v}$ as the total (base flow and disturbance) velocity and τ as the total stress in the polymeric fluid. The FENE-P viscoelastic fluid has the advantage of being similarly easy to simulate, but also including a finite extensibility for the polymers. This leads to a stress which depends on a conformation tensor ($\mathbf{C}$) for the polymer dumbbells via a non-linear spring force:

$$\tau = \frac{1-\frac{3}{L^2}}{1+\frac{L^2}{tr(\mathbf{C^2})}} \tag{1.7}$$

Again, we used Gauss-Labatto points in the wall normal direction and Fourier modes in the streamwise direction.

2. A purely elastic instability

At low Reynolds number, low β and sufficiently large Weissenberg number we observe an instability across a range of streamwise disturbance wavenumbers. This leads us to suppose that this instability might be a plausible cause for a self-sustaining process in viscoelastic plane Couette flow, similar to that observed by Waleffe.

The instability remains unchanged under variation of Δ at low Δ, proving that it is a free shear instability. Although the instability appears to require some inertia in the fluid, it is still present for $Re = 0.01$, far lower than the usual threshold of $Re = 1000$ for a Newtonian Kelvin-Helmholtz instability.

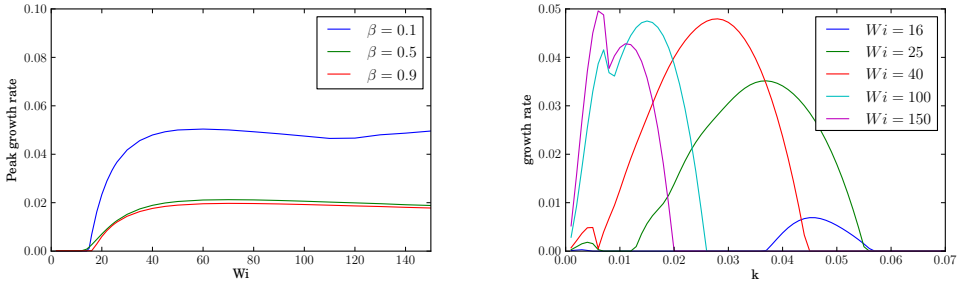

(a) (b)

Figure 2: a) Free shear version of the instability. Plot of the maximum growth rate against Wiessenberg number at $Re = 0.01$. b) Dispersion relations at various Weissenberg numbers to accompany the trend in figure a).

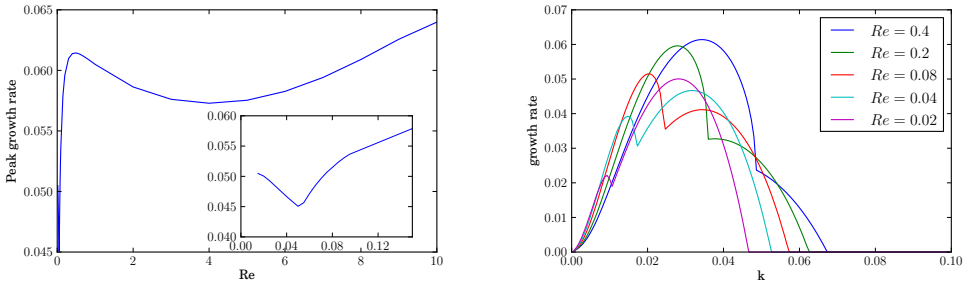

(a) (b)

Figure 3: a) Free shear version of the instability. Plot of the maximum growth rate against Reynold's number with $Wi = 50$. b) Dispersion relations at various Reynold's numbers to accompany the trend in figure a).

We see an instability grow from around $k \sim 0.06$ and move to lower k as the Weissenberg number increases (figure 2b). The height of the instability also increases with increasing Weissenberg number (figure 2a).

The dispersion relation saturates at $Wi \sim 50$ and remains approximately constant with increasing Weissenberg number. The dispersion relation for the instability remains broad in k until $Wi \sim 100$ where a new eigenvector becomes dominant.

As the Reynold's number is reduced, new eigenvalues become dominant. Although the dominant eigenvalue changes the flow is still unstable, even down to $Re = 0.01$ (see figures 3a and 3b).

2.1. *Shear instability with walls*

If we examine the eigenvectors of the instability, we see that there are very large polymer stresses in the $\pm\Delta$ region. This corresponds to the large shear rate brought about as the two flows pass each other. Examining the flow field, we see that there are large vortices arranged with opposite rotational directions above and below the shear region which extend almost to the walls.

Dependence of the instability on the channel walls persists at very small Δ. We believe that this is due to the inertial effects at low Reynold's number being so weak. This means it is very easy to move the fluid even at the shear rate present far from the centre of the

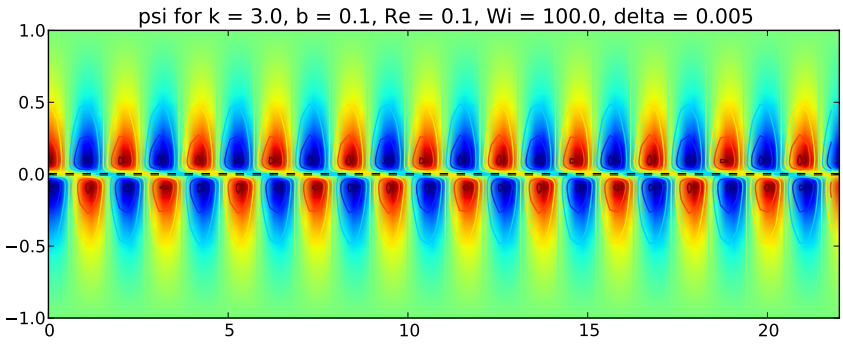

(a)

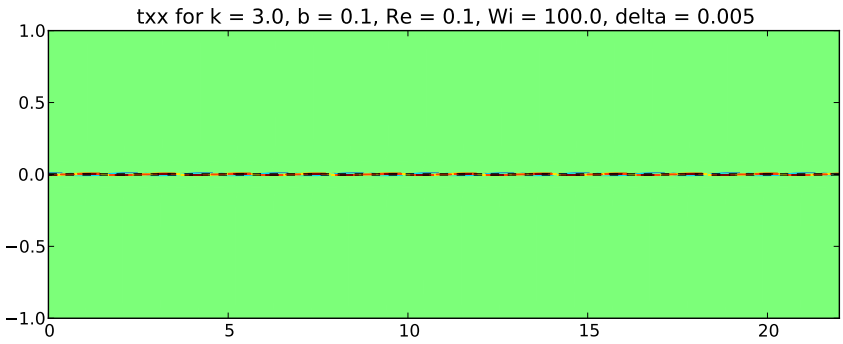

(b)

Figure 4: a) Streamfunction of the largest eigenfunction of the instability when $Re = 0.1$, $Wi = 100$, $\Delta = 0.005$. Red is positive (streamlines of the flow point clockwise around the contours), Blue is negative (streamlines of the flow point anticlockwise around the contours) b) xx stress for the same instability.

channel. I think the instability generated by the elasticity of the fluid needs the walls to dampen it for some reason.

It is difficult to see the instability at $Re = 0$. As the Reynold's number is reduced the walls become more important to the instability. In order to remove the dependence on the walls and recover a free shear instability it is necessary to move them further away. This problem gets worse at lower Re. By introducing just a very small contribution from inertia, we can remove the dependence on the walls. This is why all of our results are taken for $Re \leqslant 0.1$ on the length scale of the instability.

The reason we have have the simulation with the walls at all is because of the implications for the plane Couette problem. The Kelvin-Helmholtz instability in the Newtonian problem takes place on a length scale of about 10% of the width of the channel, or $\Delta = 0.1$ (a guess). The viscoelastic Kelvin-Helmholtz instability is sensitive to the walls at this Δ and a $Re \lesssim 1$ (see figure 7). This means that on the scale of the channel, $Re \gtrsim 10$

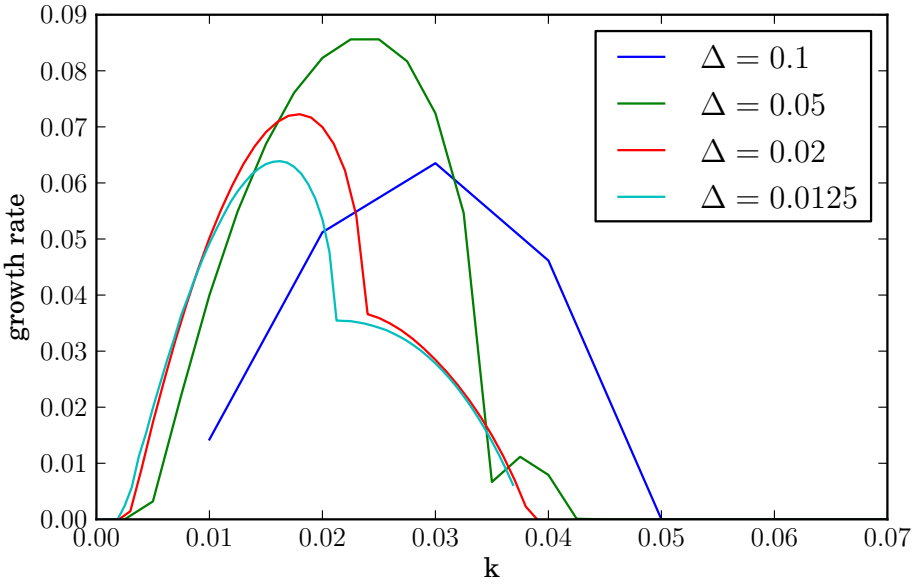

Figure 5: Dispersion relations for various values of Δ at $Re = 0.1$, $Wi = 100$. The sensitivity to the walls seems only to increase the strength of the instability. Even when the system is insensitive to the walls, at $\Delta = 0.0125$, there is still an instability present.

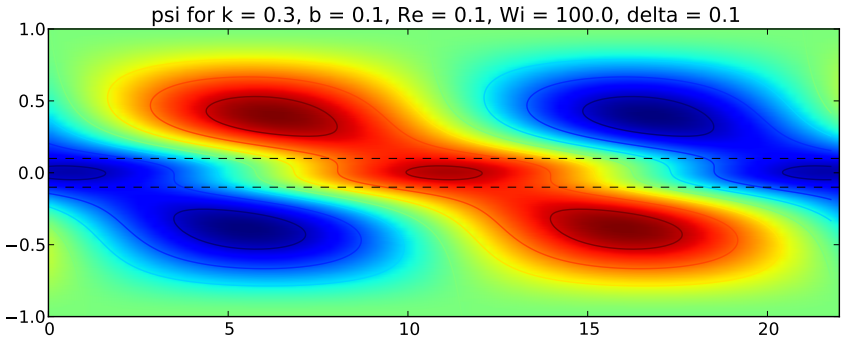

Figure 6: Streamfunction of the eigenfunction of the instability at $\Delta = 0.1$, $Wi = 100$, $Re = 0.1$. The magnitude is scaled by the xx stress in the centre of the channel.

for the walls not to affect the instability. So, the important results for the purely elastic instability from the point of view of the plane Couette problem are probably those for which the walls are relevant.

At $\Delta = 0.1$ we see the same instability as that seen in the completely free case.

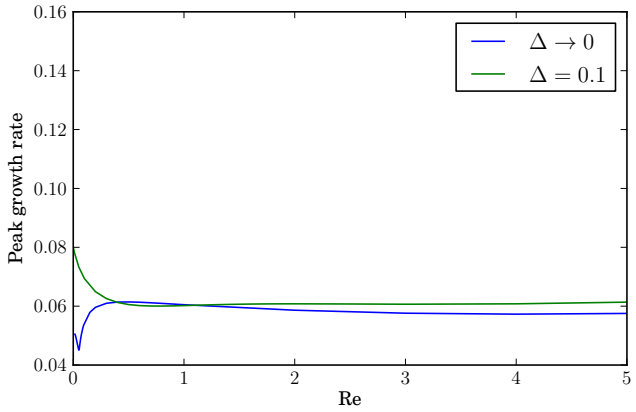

Figure 7: The blue line is the data from the stretched code and the green line is the $\Delta = 0.1$ data. By $Re = 1$ it is clear that the Reynold's number is sufficient such that the walled system behaves as though it were insensitive to the walls.

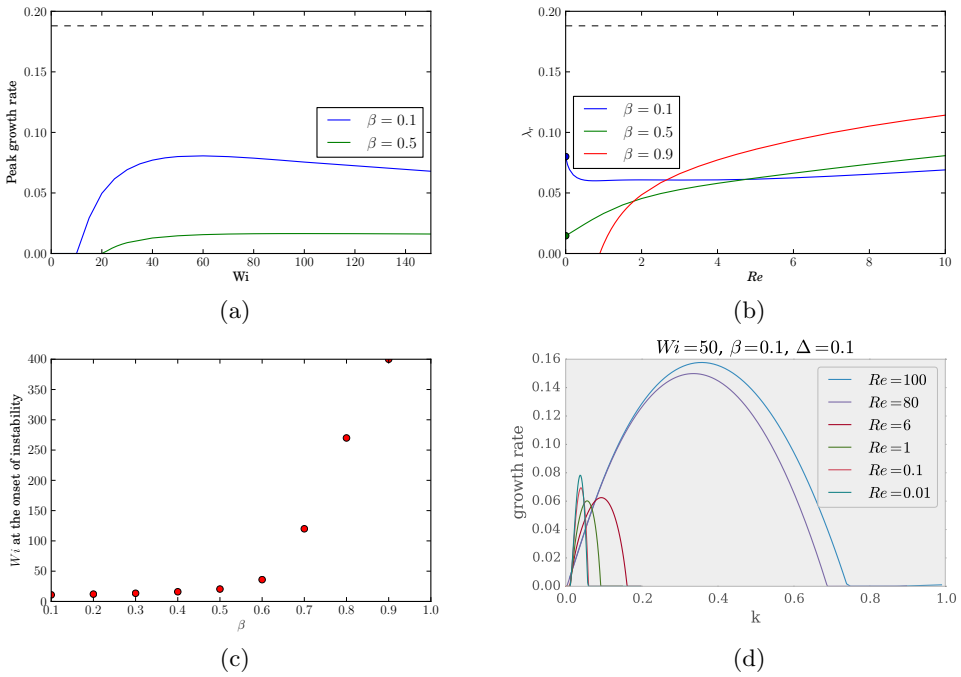

Figure 8: a) The change in the height of the dispersion relation as Wi is increased at $Re = 0$ with $\Delta = 0.1$. This instability must be entirely elastic in nature. b) The change in the height of the dispersion relation as the Reynolds number is reduced at $Wi = 5$. At low Re the instability is clearly still present for large polymer concentrations, consistent with purely elastic turbulence with $\Delta = 0.1$. c) The value of the Weissenberg number at which the velocity profile becomes unstable against β at $\Delta = 0.1$. The onset of the purely elastic instability moves to higher Wi as β increases. d) Dispersion relations at Wi =50 for $\Delta = 0.1$.

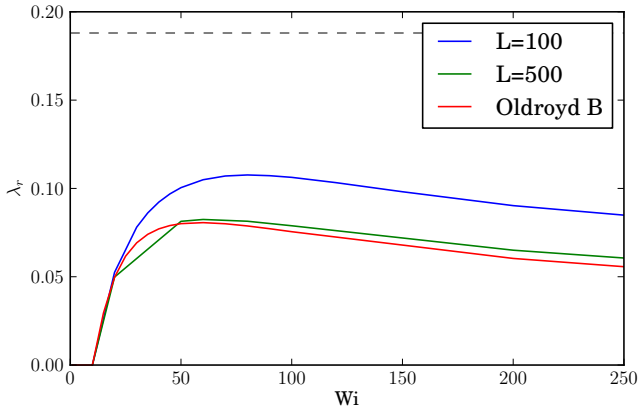

Figure 9: The FENE-P model fluid at $Re = 0$ when $\Delta = 0.1$. Results are consistent with figure 8a.

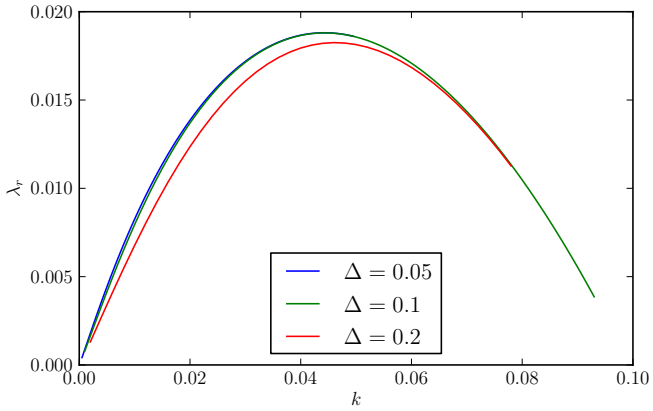

Figure 10: Dispersion relations for various values of Δ and $Re = 1000$, $Wi = 0.01$. When results are rescaled for delta, The instability is found to be insensitive to the width of the instability relative to the wall at this combination of Reynold's number and Wiessenberg number.

3. Confirming the model

3.1. *Consistency of results with the FENE model*

The finite extensibility version of the model gives good agreement with the Oldroyd-B version. Shorter lengths bring about a larger instability but do not delay it to higher Weissenberg number. Otherwise similar dispersion relations are observed with a similar dependence on the distance to the walls (figure 9).

3.2. *Varying width of the instability*

3.3. *Drag reduction*

We see drag reduction using the Oldroyd-B model. It is not clear whether or not the maximum drag reduction asymptote is present (figure 11).

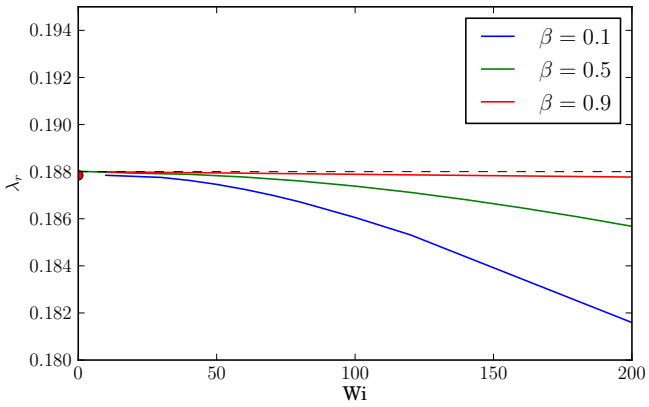

Figure 11: Peak growth rate against Wiessenberg number at $Re = 1000$, $\Delta = 0.1$ The height of the dispersion relation is reduced for the Kelvin-Helmholtz instability as the Weissenberg number is increased. The grey dashed line is the height of the dispersion relation for the Newtonian fluid. The decrease in λ_r corresponds to increased stability of the base flow and so confirms the presence of drag reduction in this system.

4. Outline of the mechanism

5. Conclusions

In conclusion, we can say that there is a Kelvin-Helmholtz like instability for purely elastic shear flows. The unstable region is much larger than that seen in Newtonian fluids relative to the region of shear. The wavenumber of the instability is much smaller in the viscoelastic case ($k < 0.06$), suggesting a larger minimal flow unit is required in viscoelastic fluids. This instability is enhanced slightly by introducing a finite extensibility to the polymers but remains of essentially the same form. The instability has grown to its maximum by the time it reaches an effective Weissenberg number $Wi \sim 50$ after which it is saturated. The instability is also strongly dependent on the walls at low effective Reynold's number.

REFERENCES

Groisman, A. & Steinberg, V. 2000 Elastic turbulence in a polymer solution flow. *Nature* **405** (6782), 53–5.

Larson, R. G., Shaqfeh, Eric S. G. & Muller, S. J. 1990 A purely elastic instability in Taylor Couette flow. *Journal of Fluid Mechanics* **218**, 573.

Toms, B. A. 1977 On the early experiments on drag reduction by polymers. *Physics of Fluids* **20** (10), S3.

Waleffe, Fabian 1997 On a self-sustaining process in shear flows. *Physics of Fluids* **9** (4), 883.

Waleffe, Fabian 1998 Three-Dimensional Coherent States in Plane Shear Flows. *Physical Review Letters* **81** (19), 4140–4143.